Pergamon

Ocean Engineering 29 (2002) 1929–1943

OCEAN ENGINEERING

www.elsevier.com/locate/oceaneng

Distribution of nonlinear wave crests

J. Al-Humoud, M.A. Tayfun *, H. Askar

Civil Engineering Department, College of Engineering and Petroleum, Kuwait University, PO Box 5969, Safat 13060, Kuwait

Received 8 June 2001; accepted 3 October 2001

Abstract

The distribution of nonlinear wave crests is examined on the basis of a theoretical probability density previously given elsewhere (J. Eng. Mech. 120 (1994) 1009). Certain errors contained in the original theoretical density are corrected, and the corresponding exceedance distribution is derived. The resulting theoretical forms of the probability density and exceedance distribution are then slightly simplified and compared with nonlinear wave data gathered under hurricane conditions. The results indicate that the proposed theoretical forms describe the observed distributions of large wave crests better than the Rayleigh law. However, the quantitative accuracy of the predictions is somewhat poor, as is typical of approximate theories based on Gram–Charlier-type expansions. © 2002 Elsevier Science Ltd. All rights reserved.

Keywords: Nonlinear waves; Wave envelope; Wave crests; Probability density; Exceedance probability

1. Introduction

The vertically skewed profile of nonlinear waves is characterized by higher, more pointed crests and shallower, more rounded troughs. An accurate prediction of these features has theoretical importance and practical relevance in ocean engineering design. In particular, the distribution of nonlinear crests coupled with stillwater levels would be a principal factor affecting the freeboard design levels, and also wave-induced runup and overtopping of structures.

The exact theoretical form of the distribution of nonlinear wave crests is not known under a general setting involving directional waves and wave spectra representative

* Corresponding author. Tel.: +965-562-7291; fax: +965-481-7524.
E-mail address: tayfun@civil.kuniv.edu.kw (M.A. Tayfun).

PII: S0029-8018(01)00101-9

of wind-generated seas. A theoretical approximation based on Edgeworth's form of the Gram–Charlier distribution was derived some years ago by Longuet-Higgins (1964). The approximation requires knowledge of six third-order joint cumulants of the surface elevation, its first and second time derivatives. The complicated theoretical forms of these cumulants and the intricacies of estimating them from actual measurements have so far rendered the Longuet-Higgins (1964) result too difficult to explore either theoretically or practically. Nonetheless, the two leading terms of the nonlinear approximation correspond identically to those of Cartwright and Longuet-Higgins (1956) in the linear case, as would be expected. However, in the narrow-band limit, the nonlinear corrections vanish, and the Rayleigh density appropriate to linear waves is obtained. This result is somewhat unexpected since it tends to contradict observations and also other relatively more recent theoretical models (Tayfun 1980, 1986; Huang et al., 1983; Langley, 1987; Tayfun and Lo, 1988; Dawson et al., 1993; Kriebel and Dawson, 1993a,b; Askar and Tayfun, 1999; Jha and Winterstein, 2000).

Several theoretical and/or empirical approximations currently exist for describing the distribution of nonlinear wave crests. Approximations based on the narrow-band model of sea waves (Tayfun 1980, 1986) include those described by Huang et al. (1983), Dawson et al. (1993), Kriebel and Dawson (1993a,b), Askar and Tayfun (1999), and others. Some of these seem particularly useful for describing the distribution of laboratory-generated wave crests (Dawson et al., 1993; Kriebel and Dawson, 1993a,b). Others appear to do somewhat better for oceanic observations (Askar and Tayfun, 1999; Jha and Winterstein, 2000). Laboratory-generated data typically display far more pronounced skewness and kurtosis values than oceanic data (Huang et al., 1983; Jha and Winterstein, 2000), possibly due to the presence of side walls, reflections, and scale effects.

More recently, the use of a Gram–Charlier type of distribution has led Tayfun (1994) to derive a number of theoretical results on nonlinear wave envelopes and phases without any restrictive assumptions concerning the directional or spectral properties of waves. The relative validity of these theoretical results was demonstrated for nonlinear wave envelopes and phases through comparisons with empirical data. Theoretical forms of the probability densities of upper and lower envelopes over the crest and through segments of the surface profile were also derived, but not compared with data. In the following, these are re-examined briefly, correcting certain algebraic errors in the original expressions. The corresponding exceedance distributions are derived, indicating how these and the associated densities can be simplified further. Subsequently, the resulting theoretical forms for nonlinear wave crests are compared with measurements gathered during hurricane Camille in the Gulf of Mexico in 1969.

2. Review of previous theory and corrections

The nonlinear surface elevation from the mean-zero level is described as a function of time t by (Tayfun, 1994):

$$\eta(t) = A(t)\cos\phi(t) \tag{1}$$

where A represents the random amplitude or envelope function, and $\phi(t)$ the random phase. Within the context of second-order nonlinear wave theory and under general conditions in deep water, the joint density of the scaled envelope $\zeta = A/A_{\mathrm{rms}}$ and ϕ has the form:

$$p(\zeta,\phi) = \frac{1}{2\pi}\left[1 + \frac{\sqrt{2}}{3}\lambda_3\zeta(\zeta^2-2)\cos\phi\right]p(\zeta) \tag{2}$$

where $\zeta\geq 0$, $0\leq\phi < 2\pi$, λ_3 is the skewness coefficient of η, and

$$p(\zeta) = 2\zeta\exp(-\zeta^2) \tag{3}$$

corresponds to the Rayleigh density. Further, $A_{\mathrm{rms}} = (2m_0)^{1/2}$ with m_0 being the zero-order spectral moment, or simply the variance of η.

Various aspects of these results have previously been discussed by Tayfun (1994). It will suffice here to reiterate that A is Rayleigh distributed as in Eq. (3), but the marginal density of ϕ is given by:

$$p(\phi) = \frac{1}{2\pi}\left(1-\frac{1}{6}\sqrt{\frac{\pi}{2}}\lambda_3\cos\phi\right) \tag{4}$$

In addition, wave crests or segments where $\eta > 0$ correspond to $0\leq\phi\leq\pi/2$ and $3\pi/2\leq\phi\leq 2\pi$ in Eq. (1). Similarly, segments or wave troughs where $\eta < 0$ coincide with $\pi/2\leq\phi\leq 3\pi/2$. Clearly, as $\lambda_3\rightarrow 0$, then $p(\phi)\rightarrow 1/2\pi$ appropriate to linear waves.

For linear waves, the surface profile is equally likely both above and below the mean-zero level. This is not so in the nonlinear case due to the vertical asymmetry of the wave profile. The time during which the profile stays above the mean-zero level is slightly shorter than that for which it is below the mean-zero level. The corresponding probabilities, say $P(+) = \mathrm{Prob}\,(\eta > 0)$ for which $0\leq\phi\leq\pi/2$ and $3\pi/2\leq\phi\leq 2\pi$, and $P(-) = \mathrm{Prob}\,(\eta < 0)$ for which $\pi/2\leq\phi\leq 3\pi/2$, follow by integration from Eq. (4) as

$$P(\pm) = \frac{1}{2}\left(1\mp\frac{\lambda_3}{3\sqrt{2\pi}}\right) \tag{5}$$

Again, as $\lambda_3\rightarrow 0$, then $P(\pm)\rightarrow 1/2$, as is expected. In general, however, $P(+) < 1/2$ and $P(-) > 1/2$ so that $P(+) + P(-) = 1$.

The conditional densities of ζ, given that $\eta > 0$ or $\eta < 0$, will be defined as $p^{+}(\zeta)$ and $p^{-}(\zeta)$, respectively. These serve to describe the distribution of ζ over the crest and through segments. Their theoretical forms routinely follow from equations (48a) and (48b) of Tayfun (1994) as

$$p^{\pm}(\zeta) = \frac{1\pm c_1\lambda_3\zeta(\zeta^2-2)}{1\mp c_0\lambda_3}p(\zeta) \tag{6}$$

where, for simplicity

$$c_0 = \frac{1}{3\sqrt{2\pi}}, \; c_1 = \frac{2\sqrt{2}}{3\pi} \tag{7}$$

are the corrections required in $p^{\pm}$ of Tayfun (1994). Also note that as $\lambda_3 \rightarrow 0$, then $p^{\pm} \rightarrow p$, as should be the case for linear waves. The theoretical forms of p^{+} of interest here are illustrated in Fig. 1 for $\lambda_3 = 0.0$, 0.1, 0.2 and 0.3. The case $\lambda_3 = 0.0$ is identical with the Rayleigh density p given by Eq. (3). For $\lambda_3 > 0$, p^{+} deviates from p noticeably, showing an excess toward the large ζ values and a corresponding deficiency over the mid-range. These features seem consistent with the vertically skewed wave profile characterized by higher and more pointed crests.

The mean and mean-square values associated with $p^{\pm}$ are given in a corrected form by

$$< \zeta >^{\pm} = \frac{1}{1 \mp c_0\lambda_3} \frac{\sqrt{\pi}}{2} \tag{8}$$

$$< \zeta^2 >^{\pm} = \frac{1 \pm c_2\phi_3}{1 \mp c_0\lambda_3} \tag{9}$$

where $c_2 = 1/8\sqrt{2}$. Again, note that as $\lambda_3 \rightarrow 0$, then $< \zeta >^{\pm} \rightarrow < \zeta > = \sqrt{\pi}/2$ and $< \zeta^2 >^{\pm} \rightarrow < \zeta^2 > = 1$ appropriate to the linear case.

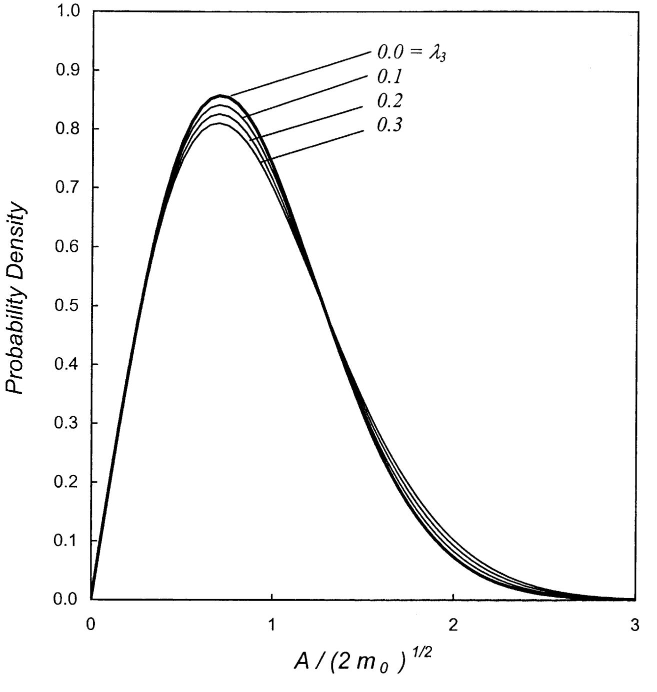

Fig. 1. Theoretical probability density p^{+} given by Eq. (6) for various λ_3. Case $\lambda_3 = 0.0$ (heavy curve) coincides with the Rayleigh form of Eq. (3).

3. Exceedance distributions and approximations

The exceedance distribution $E = \text{Prob}\,(A/A_{\text{rms}} > \zeta)$ corresponding to p^+ or p^- follows by integration from Eq. (6) as

$$E^{\pm}(\zeta) = \frac{1 \pm c_1\lambda_3\zeta\left(\zeta^2-\frac{1}{2}\right)\mp c_0\lambda_3\,\text{erfc}(\zeta)\exp(\zeta^2)}{1\mp c_0\lambda_3}E(\zeta) \tag{10}$$

where $\zeta \geq 0$, erfc() is the standard complimentary error function, and

$$E(\zeta) = \exp(-\zeta^2) \tag{11}$$

As $\lambda_3 \to 0$, then $E^+ \to E$, i.e. the Rayleigh form of the exceedance distribution in the linear case. For the general case $\lambda_3 > 0$, it can be shown that $E^+ > E$ and $E^- < E$ always for any $\zeta > 0$. The theoretical forms of E^+ are shown in Fig. 2 for the same λ_3 values as those in Fig. 1.

Many of the expressions above can be rewritten in slightly simplified forms, using the expansion

$$\frac{1}{1\mp c_0\lambda_3} = 1 \pm c_0\lambda_3 + O(\lambda_3^2) \tag{12}$$

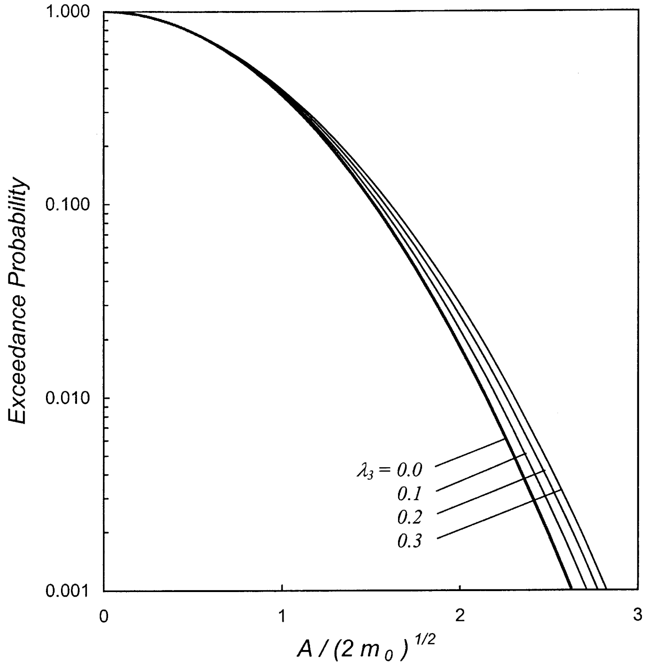

Fig. 2. Theoretical exceedance probability E^+ given by Eq. (10) for various λ_3. Case $\lambda_3 = 0.0$ (heavy curve) coincides with the Rayleigh form of Eq. (11).

In particular,

$$p^{\pm}(\zeta) = [1 \pm c_0\lambda_3 \pm c_1\lambda_3\zeta(\zeta^2-2)]p(\zeta) \tag{13}$$

$$E^{\pm}(\zeta) = \left[1 \pm c_0\lambda_3 \pm c_1\lambda_3\zeta\left(\zeta^2-\frac{1}{2}\right) \mp c_0\lambda_3 \operatorname{erfc}(\zeta)\exp(\zeta^2)\right]E(\zeta) \tag{14}$$

correct to $O(\lambda_3)$. Numerical computations indicate that these are essentially identical to Eqs. (6) and (10) for $0 < \lambda_3 < 0.3$ as a typical range of values in deep water.

For linear waves, the Rayleigh density p describes the distribution of wave envelopes in the most general case. By definition, envelope elevations always equal or exceed the surface elevations, including the positive maxima or wave crests. The distribution of positive maxima is more complicated and also slightly shifted toward lower values as compared to those implied by the Rayleigh form (Rice, 1944; Cartwright and Longuet-Higgins, 1956). On this basis, the corresponding exceedance distribution E represents an upper bound to the distribution of crest amplitudes of linear waves. Furthermore, because the wave envelope passes through all maxima exactly in the narrow-band limit, the distribution of crest amplitudes converges to the Rayleigh form. Thus, E is in fact a least upper bound to the distribution of wave crests in general, irrespective of bandwidth considerations.

In the most general nonlinear case, no exact results similar to those of Rice (1944) or Cartwright and Longuet-Higgins (1956) exist. In the narrow-band limit, the density p^+ and the corresponding E^+ should serve to describe the distribution of wave crests approximately, as was suggested previously in Tayfun (1994). In general, if p^+ and E^+ were exact, then it would be correct to expect E^+ to behave as a least upper bound to the distribution of nonlinear wave crests. Unfortunately, both are approximations since the underlying model, namely Eq. (2), is based on a truncated form of the Gram–Charlier distribution of η and its Hilbert transform (Tayfun, 1994).

4. Comparisons with data

The wave data utilized in the present comparisons were collected with the Ocean Data Gathering Program during hurricane Camille in the Gulf of Mexico on August 17, 1969 (Hamilton and Ward, 1974). Camille was an intense storm, with maximum wind speeds in excess of 300 km/h, moving toward the measurement site, station 1—South Pass 62A. The wave field was non-stationary, building up and reaching an extreme as the hurricane approached the site. Before the eventual failure of the wave gauge, some wave heights become as large as 22 m, with crest elevations rising nearly to 14 m above the mean-zero level. In view of its extreme nature, these data are ideally suited for testing the relative validity of some of the theoretical approximations here.

In the present comparisons, measurements covering three consecutive hourly segments, namely files designated as camwave.13, 14 and 15 are considered. These yield a time series of 10 800 surface elevations digitized at a constant sampling interval of 1 s and represent the most extreme conditions preceding the failure of

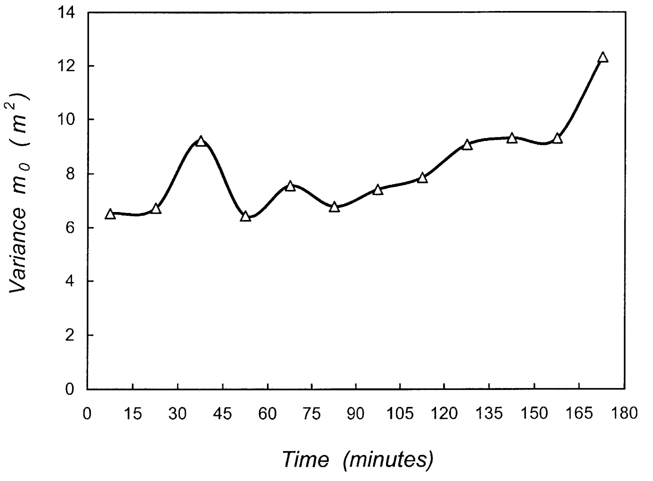

Fig. 3. Variation in the estimates of m_0 with time for camwave.13, 14 and 15 combined, and computed from 15-minute segments.

the wave gauge. The data segment was initially split into twelve 15-minute sections. These shorter data were then used to estimate the two parameters m_0 and λ_3 segmentally, as shown in Figs. 3 and 4 respectively. The non-stationarity of the wave field is evident in both of these figures. Non-stationarity in terms of m_0 does not present a major problem in this case since crests are scaled by $(2m_0)^{1/2}$, using the segmental m_0. However, the same rationale does not apply to λ_3. All theoretical expressions critically depend on the actual segmental λ_3 values. Thus, only segments with nearly

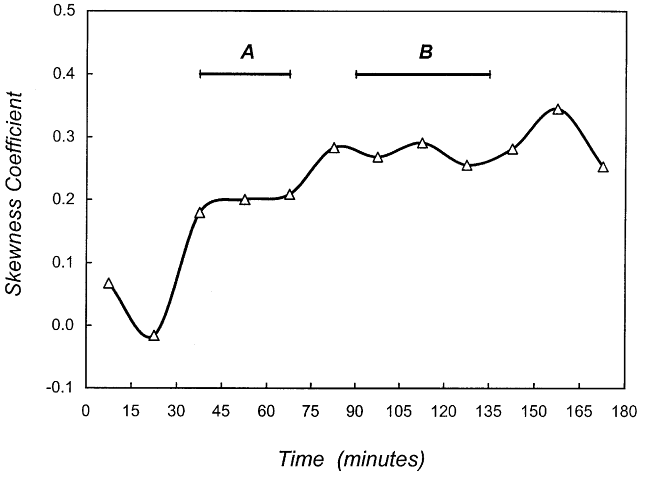

Fig. 4. Variation in the estimates of λ_3 with time for camwave.13, 14, and 15 combined, and computed from 15-minute segments. The composite data segments to be used in comparisons of p^+ and E^+ are indicated as A and B.

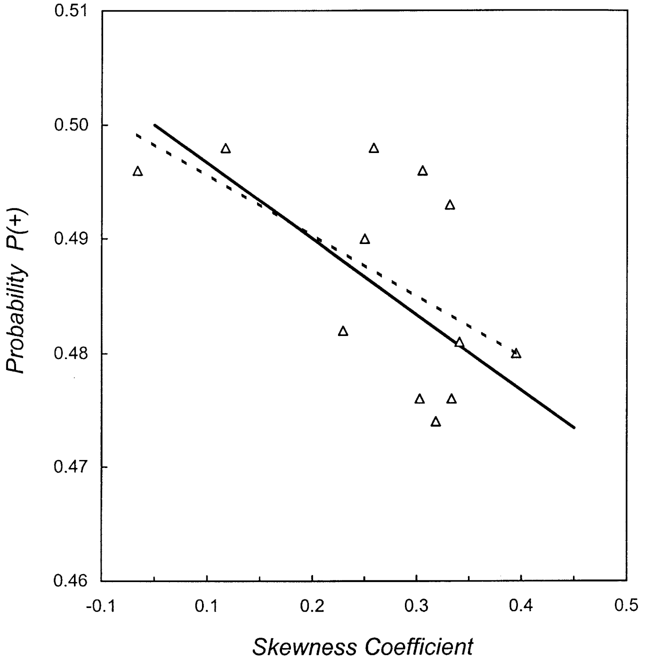

Fig. 5. Probability $P(+) = \text{Prob}\,(\eta > 0)$ versus λ_3. The solid line is Eq. (5), and the points are the empirical data estimated from 15-minute segments of camwave.13, 14 and 15 combined. The linear regression to data is dashed.

the same λ_3 values can be grouped together to enlarge the underlying data base. In the present case, two data sets shown as A and B in Fig. 4 seem to satisfy this requirement, and so will be used in the following comparisons.

The observed parameters of the composite data sets A and B are summarized in Table 1. Crest counts in both cases include all positive local maxima rather than just the largest value in a given crest segment. Clearly, set A comprises two consecutive 15-minute segments, and set B three 15-minute segments. The parameter m_0 varies for each 15-minute segment, as can be seen in Fig. 3. Thus, the crest elevations were scaled by $(2m_0)^{1/2}$ based on the 15-minute segmental m_0 values for both data

Table 1
Observed parameters of composite data sets A and B

Data set	Length (s)	Wave count[a]	Crest count[b]	m_0 (m^2)	λ_3
A	1800	181	226	7.444	0.196
B	2700	283	323	8.120	0.272

[a]Same as wave crest count for comparisons based on ‘filtered’ data.
[b]Includes all positive maxima or crests.

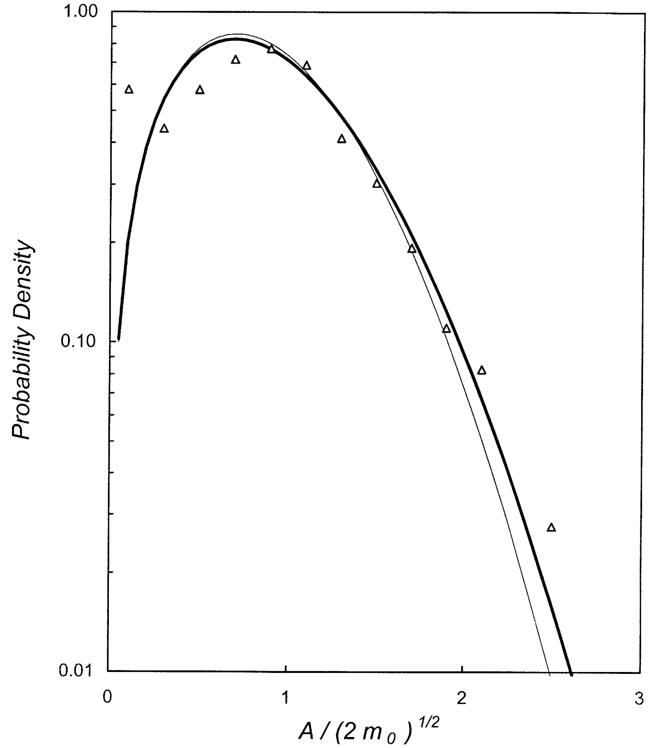

Fig. 6. Comparison between the probability density p^{+} (heavy curve, $\lambda_3 = 0.196$), Rayleigh density p (light curve), and estimates from the composite data set A (points) including all positive maxima or crests.

sets A and B. Table 1 lists only the average m_0 values representative of the whole data set A or B. The observed values of λ_3 computed from 15-minute segments do not vary appreciably from the average λ_3 values listed in the table for either set A or B, as Fig. 4 illustrates.

The comparison between $P(+) = \text{Prob}\ (\eta > 0)$ given by Eq. (5) and the empirical values computed from 15-minute segments is shown in Fig. 5. The same figure also contains the linear regression implied by the empirical points. In this case, the theoretical approximation predicts the empirical values fairly well relative to the regression line.

The comparisons between the theoretical density p^{+} and the observed values are shown in Figs. 6 and 7 for data sets A and B, respectively. The Rayleigh density p is also included in both of these figures. In both cases, the approximate theory p^{+} compares more favorably with the data, particularly over the mid-range and also toward the large wave tail. The comparisons between the theoretical exceedance distribution E^{+} and the observed data are given in Figs. 8 and 9, together with the Rayleigh form E. In both cases, the Rayleigh curve underpredicts the observed crests in a pronounced manner over the large-wave range. The approximation E^{+} does

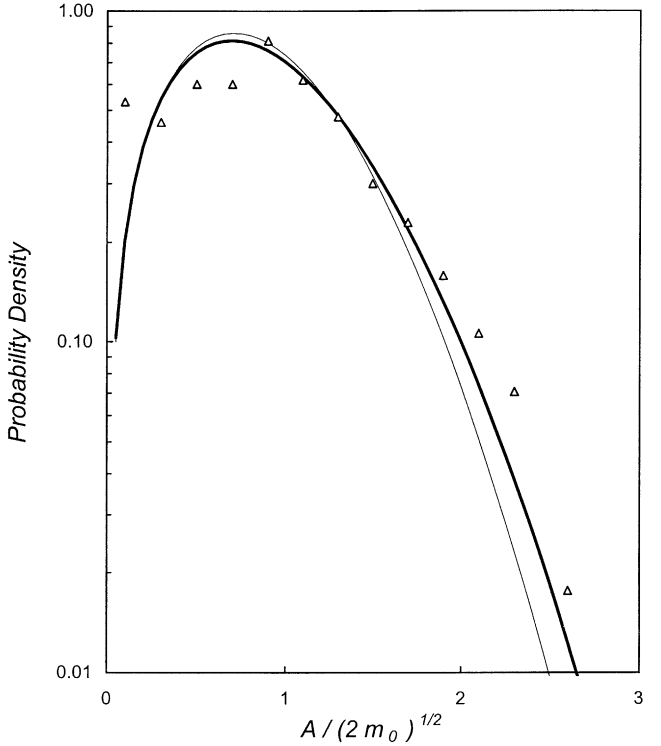

Fig. 7. Comparison between the probability density p^{+} (heavy curve, $\lambda_3 = 0.272$), Rayleigh density p (light curve), and estimates from the composite data set B (points) including all positive maxima or crests.

noticeably better over the same range, but still underestimates the large crests somewhat.

To explore the effect of excluding secondary crests, the theoretical curves E and E^{+} of Figs. 8 and 9 were reproduced in Figs. 10 and 11, this time together with the 'filtered' data sets A and B for comparison. The filtered data set A comprises 181 crest elevations, excluding 45 (=226−181) secondary crests counted in the prior analysis. Similarly, the filtered set B contains 283 crest elevations, excluding 40 (=323−283) secondary crests. Both figures show that the data are slightly shifted toward the larger crest values. As a result, the discrepancy between the theoretical predictions and the data becomes somewhat more pronounced over the range of large waves.

5. Concluding remarks

The distribution of nonlinear wave crests based on the corrected form of a theoretical approximation previously given by Tayfun (1994) was compared with the Rayleigh theory and observed data. Comparisons suggest that the approximate nonlinear

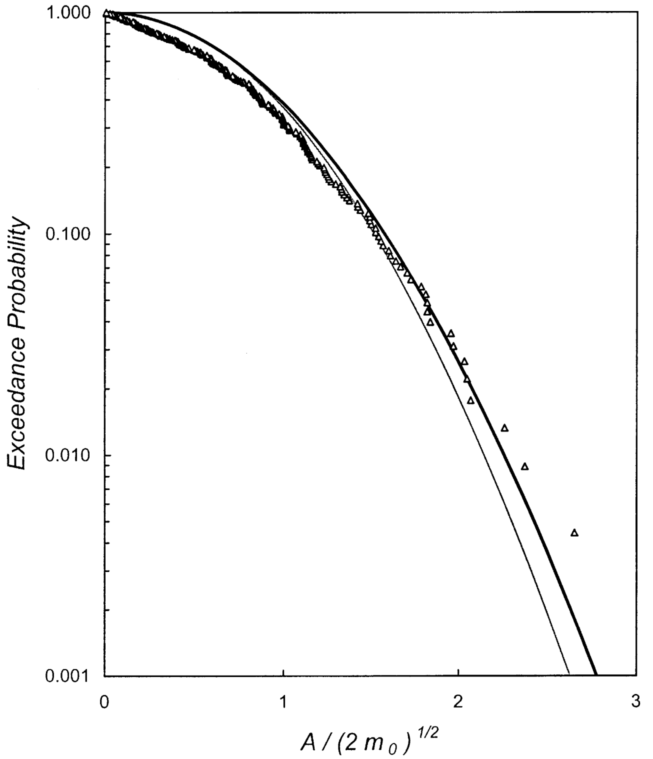

Fig. 8. Comparison between the exceedance probability E^{+} (heavy upper curve, $\lambda_3 = 0.196$), Rayleigh form E (lower curve), and estimates from the composite data set A (points) including all positive maxima or crests.

theory qualitatively describes the observed data well, particularly over the range of large waves. However, the quantitative accuracy of the predictions is not entirely satisfactory. Large wave crests of design interest are underestimated. The overall nature of these results is consistent with other approximate theories derived from a truncated form of the Gram–Charlier distribution, including those employed to describe the distribution of nonlinear surface elevations (Huang and Long, 1980; Bitner, 1980). Typically, the qualitative effects of nonlinearities are predicted well, but the quantitative comparisons with data are for the most part less than satisfactory.

The data used for the comparisons are relatively old. The sampling rate employed (1 Hz) is somewhat low, suggesting that the observed values may underestimate the actual crest elevations by 1–3% on the average. The obvious nonlinearity of the data makes them ideally suited for the present comparisons. However, the wave field is also non-stationary, making a rigorous analysis practically difficult. This was heuristically remedied in the present case by considering 15-minute segments to balance the conflicting requirements between the use of shorter time histories to avoid non-stationarity and the preference for larger samples to ensure statistical stability.

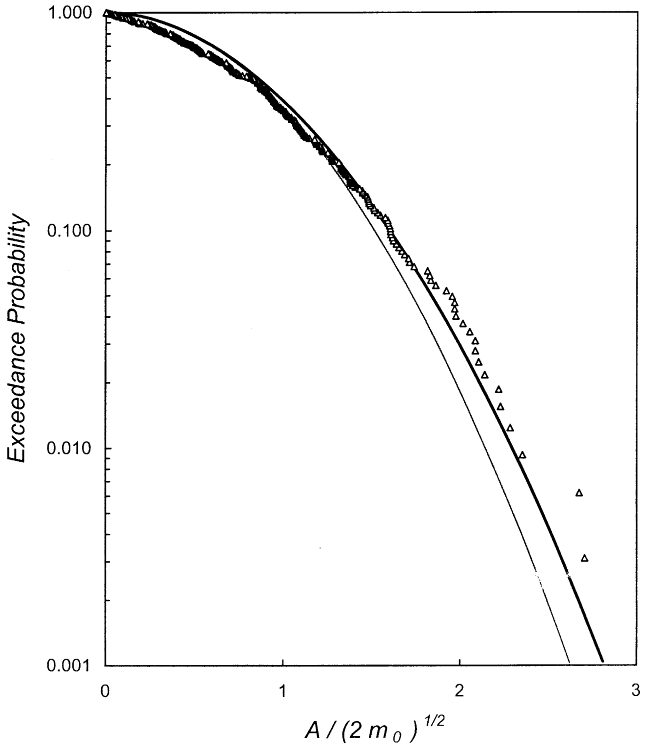

Fig. 9. Comparison between the exceedance probability E^{+} (heavy upper curve, $\lambda_3 = 0.272$), Rayleigh form E (lower curve), and estimates from the composite data set B (points) including all positive maxima or crests.

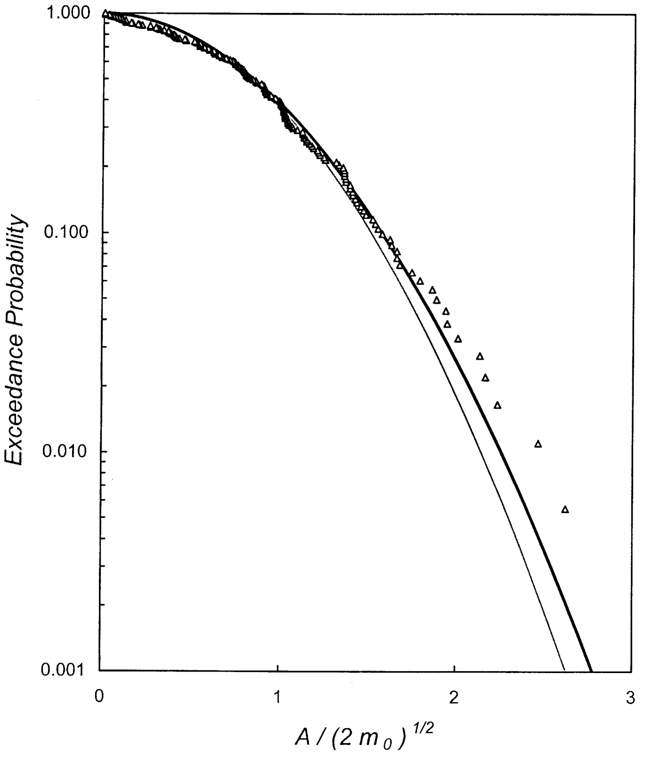

Fig. 10. Same as Fig. 8 except for the ‘filtered’ data set A, excluding secondary positive maxima from analysis.

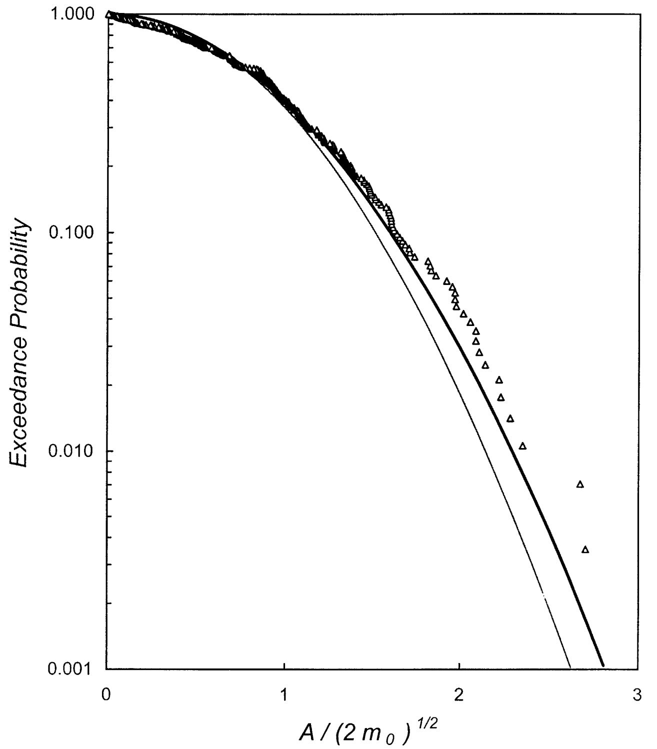

Fig. 11. Same as Fig. 9 except for the ‘filtered’ data set B, excluding secondary positive maxima from analysis.

Acknowledgements

The writers thank G.Z. Forristall for the wave data and Mini Kora for word processing.

References

Askar, H., Tayfun, M.A., 1999. Exceedance distribution of large crest heights. Kuwait Journal of Science and Engineering 26, 225–238.

Bitner, E.M., 1980. Nonlinear effects of the statistical model of shallow-water wind waves. Applied Ocean Research 2 (2), 63–73.

Cartwright, D.E., Longuet-Higgins, M.S., 1956. The statistical distribution of the maxima of a random function. Proceedings of the Royal Society of London, Series A 237, 212–337.

Dawson, T.H., Kriebel, D.L., Wallendorf, L.A., 1993. Breaking waves in laboratory-generated JONSWAP seas. Applied Ocean Research 15, 85–93.

Hamilton, R.C., Ward, E.G., 1974. Ocean data gathering program: quality and reduction of data. In: Proceedings of the Fourth Annual Offshore Technology Conference. American Institute of Mining, Meteorological and Petroleum Engineering, Houston, Texas, pp. 749–769.

Huang, N.E., Long, S.R., 1980. An experimental study of the surface elevation probability distribution and statistics of wind generated waves. Journal of Fluid Mechanics 101, 179–200.

Huang, N.E., Long, S.R., Tung, C.C., Yuen, Y., Bliven, L.F., 1983. A non-Gaussian statistical model for surface elevation of nonlinear random wave fields. Journal of Geophysical Research, American Geophysical Union 88, 7597–7606.

Jha, A.K., Winterstein, S.R., 2000. Nonlinear random ocean waves: Prediction and comparison with data. In: Proceedings of the ETCE/OMAE 2000 Joint Conference, American Society of Mechanical Engineers, paper ETCE/OMAE2000-6125.

Kriebel, D.L., Dawson, T.H., 1993a. Distribution of crest amplitudes in severe seas with breaking. Journal of Offshore Mechanics and Arctic Engineering 115, 9–15.

Kriebel, D.L., Dawson, T.H., 1993b. Nonlinearity in wave crest statistics. In: Proceedings of the Second International Conference on Wave Measurement and Analysis. American Society of Civil Engineers, New Orleans, Louisiana, pp. 61–75.

Langley, R.S., 1987. A statistical analysis of nonlinear waves. Ocean Engineering 14 (5), 389–407.

Longuet-Higgins, M.S., 1964. Modified Gaussian distributions for slightly nonlinear variables. Radio Science Journal of Research NBS/USNC-URSI 68D (9), 1049–1062.

Rice, S.O., 1944. Mathematical analysis of random noise. Reprinted in Selected Papers on Noise and Stochastic Processes, Dover Publications, 1954, pp. 132–294.

Tayfun, M.A., 1980. Narrow-band nonlinear sea waves. Journal of Geophysical Research, American Geophysical Union 85 (3), 1548–1952.

Tayfun, M.A., 1986. On narrow-band representation of ocean waves 1. Theory. Journal of Geophysical Research, American Geophysical Union 91 (C6), 7743–7752.

Tayfun, M.A., 1994. Distributions of envelope and phase in weakly nonlinear random waves. Journal of Engineering Mechanics, American Society of Civil Engineers 120 (4), 1009–1025.

Tayfun, M.A., Lo, J.-M., 1988. Envelope, phase, and narrow-band models of sea waves. Journal of Waterway, Port, Coastal and Ocean Engineering, American Society of Civil Engineers 115 (5), 594–613.